Journal of Power Sources 267 (2014) 714–722

Contents lists available at ScienceDirect

Journal of Power Sources

journal homepage: www.elsevier.com/locate/jpowsour

A facile synthesis of highly stable multiblock poly(arylene ether)s based alkaline membranes for fuel cells

Amaranadh Jasti [a, b], Vinod K. Shahi [a, b, *]

[a] Academy of Scientific and Innovative Research, India
[b] Electro-Membrane Processes Division, CSIR-Central Salt and Marine Chemicals Research Institute (CSIR-CSMCRI), G. B. Marg, Bhavnagar 364 002, Gujarat, India

HIGHLIGHTS

- Multiblock alkaline membranes are synthesized by a facile green method.
- Hydrophilic/hydrophobic phase separation causes for high conductivity.
- The presence of vicinal quaternary ammonium groups improves alkaline stability.
- Alkaline membrane for fuel cell applications.

GRAPHICAL ABSTRACT

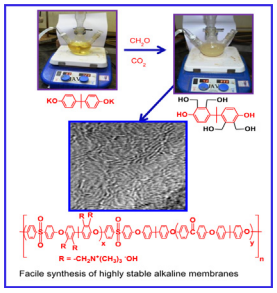

ARTICLE INFO

Article history:
Received 15 March 2014
Received in revised form
22 May 2014
Accepted 25 May 2014
Available online 4 June 2014

Keywords:
Aminated multiblock poly(arylene ether)s
Alkaline membrane
Hydrophilic/hydrophobic phase separation
Alkaline stability
Alkaline direct methanol fuel cell

ABSTRACT

Herein, we are disclosing simple route for the preparation of alkaline membranes (AMs) based on aminated multiblock poly(arylene ether)s (AMPEs) synthesized by nucleophilic substitution-poly condensation followed by quaternization and alkalization reactions. In this procedure, four quaternary ammonium groups are successfully introduced without use of carcinogenic reagents such as chloromethylmethyl ether (CMME). Hydrophilic/hydrophobic phase separation is responsible for their high hydroxide conductivity (~150 mS cm^{-1} at 80 °C) due to development of interconnected ion transport pathway. AMs are exhibiting good alkaline stability due to the presence of two vicinal quaternary ammonium groups and avoid degradation such as Sommelet–Hauser rearrangement and Hofmann elimination. Vicinal quaternary ammonium groups also resist nucleophilic (OH^-) attack and suppress the Stevens rearrangement as well as S_N2 substitution reaction due to stearic hindrance. Optimized AM (AMPE-M20N15 (55% DCM)) exhibits about 0.95 V open circuit voltage (OCV) and 48.8 mW cm^{-2} power density at 65 °C in alkaline direct methanol fuel cell (ADMFC) operation. These results suggest promising begin for the preparation of stable and conductive AMs for ADMFC applications and useful for developing hydroxide conductive materials.

1. Introduction

Fuel cells are promising renewable energy sources for automotive, stationary and mobile applications because of their high efficiency and low pollution levels [1,2]. Proton exchange membrane fuel cells (PEMFCs) have attracted significant attention during the last few years but the obstacles like fuel crossover, conductivity loss

* Corresponding author. Electro-Membrane Processes Division, CSIR-Central Salt and Marine Chemicals Research Institute (CSIR-CSMCRI), G. B. Marg, Bhavnagar 364 002, Gujarat, India. Fax: +91 0278 2566970.
E-mail addresses: vkshahi@csmcri.org, vinodshahi1@yahoo.com (V.K. Shahi).

http://dx.doi.org/10.1016/j.jpowsour.2014.05.129
0378-7753/

at elevated temperature, use of noble metal catalysts and their poisoning hampered their commercialization [2]. Alkaline direct methanol fuel cells (ADMFCs) have the potential to overcome the above problems due to good reaction kinetics, less fuel crossover (due to reverse electro-osmosis) in addition to avoid of noble metal catalysts results to high power output with low cost fuel cells [3–6]. To date, several types of AMs based on polystyrene [7], poly(-phenylene oxide) [8], poly(ether-imide) [9], radiation-grafted fluorinated polymers [10,11], organic-inorganic hybrid composites [12–14], polybenzimadazole [15,16], or poly(arylene ether)s [17–23] have been reported. Although, these AMs displayed wide range of conductivity and suitability for ADMFC applications, the membrane stability in alkaline media at elevated temperatures is poor due to aforementioned possible degradation mechanisms of quaternary ammonium groups [18,24,25].

Researchers continued to explore alternatives to circumvent this obstacle by different way of quaternization techniques. Recently, Yan et al. [26] and Zhang et al. [21] synthesized AMs based on quaternary phosphonium and benzyl quaternary guanidinium respectively with high conductivity and good alkaline stability. Further, Hickner et al. [27] reported quaternized poly(2,6-dimethyl phenylene oxide) containing long alkyl side chain pendant to the central nitrogen based AMs in order to resist nucleophilic attack but there is a possibility of ammonium groups degradation via Hofmann elimination due to presence of β-hydrogen atom on quaternary ammonium group. However, the above reported AMs have only single cationic group and can carry only one anion. On the other hand, presence of four quaternary ammonium groups has the potential to increase the ion exchange capacity and hydroxide conductivity of the membranes. Watanabe and Miyatake et al. group reported AMs based on anion conductive poly(arylene ether)s [18] and successfully introduced four cationic groups by Fridel-Crafts chloromethylation reaction using CMME but the reagent was carcinogenic and potentially harmful to human health [28–31]. Recently, Hickner et al. [32] reported quaternary ammonium functionalized benzylmethyl containing poly(arylene ether ketone)s having six quaternary ammonium groups with Br^- as counter anion. But these AMs are quite sensitive in alkaline conditions and easily undergo Sommelet–Hauser rearrangement, Stevens rearrangement and S_N2 substitution reaction due to the presence of more ortho-hydrogen and α-H atoms which causes to functional group degradation. Thus, the development of highly stable and conducting AMs by a facile green method is still an interesting challenge [33,34].

We have reported a series of AMs with well-controlled composition and structure which shows high hydroxide ion conductivity, excellent alkaline stability for ADMFCs applications by introducing four cationic groups via pre-chloromethylation of bisphenol monomer in a facile green manner. The introduction of two vicinal quaternary ammonium groups in the membrane matrix is the key part of the reported method. This imparts the membrane alkaline stability and avoids the degradations such as Sommelet–Hauser rearrangement owing to the absence of ortho hydrogen adjacent to quaternary ammonium groups. Further, Hofmann elimination was also rule out due to absence of β-hydrogen atoms. Even though the developed AMs have more α-H atoms, Stevens rearrangement and S_N2 substitution reaction has been also suppressed due to the stearic hindrance of vicinal quaternary ammonium groups. A detailed investigation on membrane properties such as water affinity, swelling ratio (%), hydroxide ion conductivity, mechanical, alkaline stability and long term durability, on membrane composition was carried out to assess the suitability of these AMs for ADMFC application.

2. Experimental section

2.1. Materials and methods

4,4′-Difluorophenyl sulfone (FPS), 4,4′-difluorobenzophenone (DFBP), and bisphenol A (BPA) were obtained from Aldrich, and crystallized in toluene/ethanol. Formaldehyde, potassium carbonate, calcium carbonate, thionyl chloride, *N*, *N*′-dimethylacetamide, toluene, methanol, 1,1,2,2-tetrachloroethane (TCE) and trimethylamine aqueous solution (35wt %) were purchased from Spectrochem, India and used as received. Chloroform, sodium hydroxide, ethanol, and acetone were (AR grade; SD Fine Chemicals, India) used as received. Nitrogen and argon gases were purchased from Ultra-Pure Gases (I) PVT. LTD., India.

2.1.1. Synthesis of 2,2′,3,3′-tetrakis(chloromethyl)bisphenol (TCMBP) monomer

A 300 mL round-bottomed flask was charged with bisphenol-A (40 mmol), K_2CO_3 (100 mmol) and water (200 mL) containing 37% formaldehyde (740 mmol) under constant stirring in an inert atmosphere at 60 °C for 4 h. CO_2 was bubbled through yellow coloured solution at 30 °C until it turned to cloudy (as shown in the photograph). The reaction mixture was extracted with ethyl acetate and dried in $MgSO_4$ followed by removal of solvent under reduced pressure. The obtained 2,2′,3,3′-tetrakis (hydroxymethyl)bisphenol (THMBP) monomer was diluted with $CHCl_3$ followed by drop-wise addition of $SOCl_2$ (120 mmol) solution in $CHCl_3$ (100 mL) over 30 min. Above solution was stirred for 1 h and washed with saturated aqueous $NaHCO_3$ to remove excess of $SOCl_2$. Now the organic layer was dried ($MgSO_4$) and solvent was removed under reduced pressure. 55% yield of 2,2′,3,3′-tetrakis(chloromethyl)bisphenol (TCMBP) monomer was obtained. The structure of obtained monomers was confirmed by ^{1}H NMR spectra. (a) THMBP (40% yield): δ 4.76 (br, 4H), 4.93 (br, 4H), 1.70 (S, 6H), 7.17 (d, 2H), 7,24 (d, 2H) and (b) TCMBP(55% yield): δ 4.61 (s, 4H), 4.74 (s, 4H), 1.53 (s, 6H), 7.00 (d, 2H), 7,06 (d, 2H).

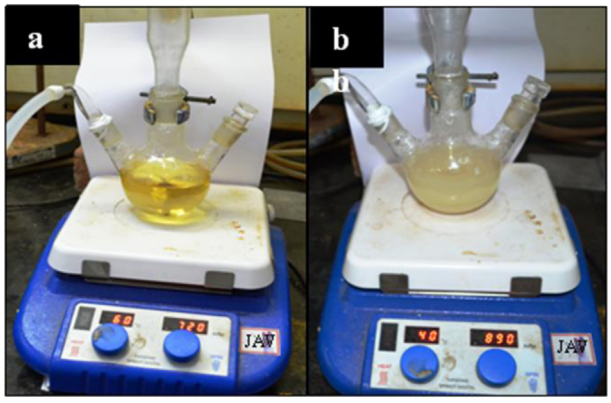

(a) Before and (b) after the gas purging

Here $SOCl_2$ is not an innocuous material; causes skin burning and eye damage. In contact with water it liberates toxic gas so it's necessary to avoid moisture in the reaction. This reagent can be handled easily with proper safety protocol.

2.1.2. Synthesis of aminated poly(arylene ether)s (AMPEs) based alkaline membranes

AMs are synthesised by nucleophilic substitution-poly condensation of TCMBP, FPS and DFBP monomers. Detailed Synthesis of aminated poly(arylene ether)s (AMPEs) based alkaline

membranes has been included in Section S1. Three types of alkaline membranes (AMPE-M20N15, AMPE-M15N15, and AMPE-M10N15 where *M* and *N* represent number of repeating unit of the hydrophilic and hydrophobic segment, respectively) were prepared by varying the block length of hydrophilic oligomers and degree of chloromethylation (DCM).

2.2. Membrane characterizations and stabilities

Detailed procedure for water uptake (*WU*), swelling ratio (%), ion exchange capacity (IEC), hydroxide conductivity (σ) and activation energy (E_a) of developed AMs has been included in Section S3. The hydrothermal and alkaline stability tests were carried by placing the AMs in a closed vial filled with the water and 8 M NaOH at 80 °C for 500 h. Changes in the chemical structure was investigated by ^{1}H NMR spectra. Membrane stabilities were evaluated by loss in IEC, and conductivity of samples. Detailed explanation of thermal and mechanical stabilities of AMs was included in Section S4.

2.2.1. Methanol permeability and selectivity parameter measurements

Methanol permeability and selectivity parameter of developed AMs were investigated and detailed procedure has been included in Section S5.

2.2.2. Preparation of membrane electrode assembly (MEA)

MEA was fabricated by our previous technique which consists of three-layer structure (AM, anode/cathode catalyst layer and diffusion layers) [40]. The carbon paper was wet proofed with 12 wt.% PTFE solution by the brush painting method. The GDL (25 cm^2 geometric area) was fabricated by coating slurry of 0.50 mg cm^{-2} consisting of carbon black (Vulcan XC72R) and PTFE dispersion on carbon paper. The Pt loading in both the anode and cathode was 0.4 mg cm^{-2}. Thus, the obtained electrode was cold pressed membrane followed by curing at 60 °C for 12 h and then hot pressed at 130 °C for 3 min at 1.2 MPa. The MEA was achieved by hot pressing an electrode/membrane/electrode sandwich at a temperature of 100 °C for 3 min at 1.0 MPa. The MEA was assembled into a single cell (FC25-01 DM fuel cell), 2 M MeOH in 6 M NaOH was used as a fuel at anode and air at the cathode and fed with 5 mL min^{-1} and 100 mL min^{-1} respectively to record the current–voltage polarization curves with the help of an MTS-150 manual fuel cell test station (ElectroChem Inc., USA). Single cell performance was carried with developed AMs (55% DCM) at 65 °C.

3. Results and discussion

3.1. Synthesis and characterization of 2,2′,3,3′-Tetrakis(chloromethyl)Bisphenol (TCMBP) monomer

TCMBP was synthesized by two steps: synthesis of 2,2′,3,3′-tetrakis(hydroxymethyl)bisphenol (THMBP); and conversion of THMBP to TCMBP using the thionyl chloride. Detailed synthesis procedure has been shown in scheme 1and investigated by ^{1}H NMR spectra. During the preparation of THMBP, another major product 2,2′,6,6′-tetra(hydroxy methyl)bisphenol monomer (50% yield) is also formed. But here, we have preferred the minor product of 2,2′,3,3′-tetra(hydroxy methyl)bisphenol monomer for the development of AMs, as it has the capability to restrict the possible degradations due to stearic hindrance generated by two bulky vicinal quaternary ammonium groups after quaternization reaction.

Two broad peaks at 4.76 and 4.93 ppm chemical shift values correspond to two asymmetric $-CH_2OH$ groups (denoted as “e” and “d”, respectively), aromatic protons (7.17–7.24 ppm) are designated as “a”, and “b”, while for $-C(CH_3)_2$ (gem-dimethyl) group (1.70 ppm) was designated as “c” in Fig. S1(a). After treatment of THMBP with $SOCl_2$; two peaks appears at 4.61 ppm & 4.74 ppm (corresponding to $-CH_2Cl$ group and denoted as “4” and “5” respectively) due to shielding effect in addition to the D_2O peak (4.20 ppm). Peak for $-C(CH_3)_2$ group was aroused at 1.53 ppm (assigned as “3”), while for aromatic protons are in the range of 7.00–7.06 ppm (assigned as “1” and “2”) observed in Fig. S1(b). Chemical shift values for $-CH_2Cl$ group is marginally less in compare with $-CH_2OH$ group, because of less deshielding nature of −Cl group than −OH group. The −OH group is a strong activating group by resonance effect; if the electrophilic substitution takes place at both ortho positions of −OH groups, a single $-CH_2OH$ peak along with one aromatic singlet peak should only appear. But from the ^{1}H NMR spectrum of THMBP, there were two $-CH_2OH$ peaks observed along with a double doublet of two dissimilar aromatic protons appeared to be merged. These observations confirmed electrophilic substitution at both ortho-positions of −OH and $-C(CH_3)_2$ groups (caused by the activating nature of $-C(CH_3)_2$ group by inductive effect).

The degree of chloromethylation (DCM) for TCMBP was estimated by ^{1}H NMR spectra by the integral peaks ratio of “4”, and “5” (assigned for $-CH_2Cl$ group) to those of peak 3 (assigned for $-C(CH_3)_2$ group) by following expression.

$$\mathrm{DCM} = \frac{2A(H_4 + H_5)}{A(H_3)} \quad (1)$$

Where A (H_4 + H_5) is the sum of integral area of both H_4 and H_5 peaks (assigned for $-CH_2Cl$ group), and A (H_3) is the area of the H_3 peak (assigned for $-C(CH_3)_2$ group) (Fig. S1(b)). TCMBPs with different DCMs (90%, 55% and 35%) were prepared by varying the molar ratios of formaldehyde and $SOCl_2$ (Table S1).

3.2. Synthesis and characterization of chloromethylated multiblock copoly(arylene ether)s (CMBPEs)

A series of CMBPEs (varied DCMs) with different hydrophilic and hydrophobic oligomer ratios were synthesized by nucleophilic substitution poly-condensation. CMBPE was designated as -M10N15, -M15N15, and -M20N15; where numbers after *M* and *N* represent the degree of polymerization for hydrophilic and hydrophobic blocks respectively (Scheme 1). The hydrophilic oligomer were prepared in dry DMAC by poly condensation of TCMBP and FPS with controlled feed monomer ratio (e.g., TCMBP/FPS = 10/11 molar ratio for an $X = 10$ oligomer) in the presence of K_2CO_3. A little amount of FPS was added at the last stage of the oligomerization reaction for the end-capping of the oligomers with F-terminal groups.

The OH-terminal bisphenol containing hydrophobic oligomers were prepared similarly with DFBP and the controlled excess amount of BPA [19]. The chemical structure and molecular weight of the hydrophilic and hydrophobic oligomers were characterized by ^{1}H NMR spectra and GPC measurements (Fig. S2 and Table S2). The oligomer lengths were determined from the ^{1}H NMR spectra by the integral ratio of protons at the terminal phenyl groups to those in the repeat units. Block copolymerization was carried out with by coalescing of different block lengths of hydrophilic and hydrophobic (BPA-containing) oligomers in the presence of K_2CO_3 and $CaCO_3$ in dry DMAc solution renders a series of CMBPEs (CMBPE -M10N15, -M15N15, and -M20N15). Since the poly condensation reaction has been carried out at below 200 °C, the cholormethyl groups does not undergo self-crosslinking reaction and remains for quaternization [35,36].

Obtained CMBPE copolymers were soluble in organic solvents such as 1,1,2,2-tetrachloroethane, dichloromethane, chloroform, DMAc, N,N-dimethylformamide (DMF), and dimethylsulfoxide (DMSO). The molecular weights of the CMBPE-M20N15 (90% DCM)

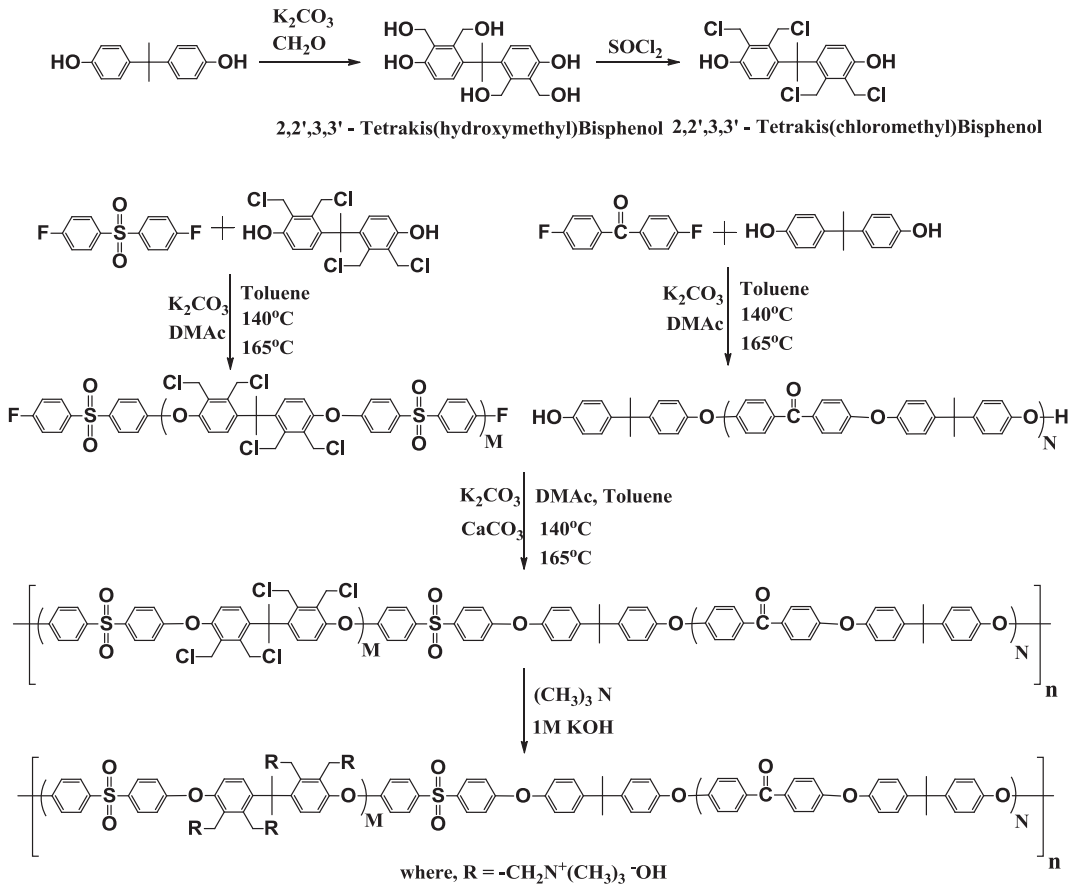

Scheme 1. Reaction scheme for the preparation of AMPE based AMs.

were estimated by GPC and summarized in Table 1. Molecular weights of CMBPEs were several times higher in compare with both (hydrophilic and hydrophobic) parental oligomers, confirmed the formation of multiblock copolymers. The ^{1}H NMR spectra of the CMBPEs were well-designated to the presumed chemical structure (Fig. 1(a) as an example for CMBPE-M20N15 (90% DCM)) by referring to the spectra of the parental oligomers (Fig. S2). The oligomer feed ratio and copolymer composition were in good agreement which supports the multiblock structure.

Peaks at 4.69 ppm and 4.74 ppm corresponding to methylene protons of chloromethyl groups (denoted as c and d). While, methyl protons of the $-C(CH_3)_2$ group (denoted as e and l respectively) showed peaks at 1.69 ppm and the aromatic protons of both hydrophilic and hydrophobic blocks along with bridged hydrocarbon unit showed peaks between 6.77 and 7.86 ppm were observed in the ^{1}H NMR spectrum of CMBPE-M20N15 (90% DCM) (Fig. 1(a)).

3.3. Membrane formation and amination of CMBPEs

Membranes were prepared by dissolving CMBPEs in 1,1,2,2-tetrachloroethane and cast the polymer solution on a clean glass plate followed by drying in a vacuum oven at 80 °C for 24 h. The dried CMBPE membrane was aminated with TMA and further immersed in 1 M KOH for alkalization at room temperature for 48 h for obtaining AMPE membranes in alkaline form.

Table 1
Molecular weights of the CMBPE (90% DCM) copolymers.

Membranes	M_n (kg mol^{-1})	M_w (kg mol^{-1})	M_w/M_n
CMBPE-M10N15	69	138	2.0
CMBPE-M15N15	57	110	1.9
CMBPE-M20N15	85	195	2.3

The peaks at 4.69 ppm and 4.73 ppm (due $-CH_2Cl$ groups) were disappeared while, new peaks at 5.27 and 5.51 ppm were observed because of the methylene groups of quaternary ammonium groups (denoted as c and d). A peak at 2.94 ppm was observed and corresponds to the $-CH_3$ groups of the quaternary ammonium groups (denoted as m). The peaks at 1.75 and 1.62 ppm were merged due to $-C(CH_3)_2$ group (denoted as l and e) and aromatic protons showed in the range of 6.82–8.06 ppm in ^{1}H NMR spectrum of AMPE-M20N15 (90% DCM) (Fig. 1(b)).

3.4. Structural morphology of AMPE membranes

TEM images of AMPE-M10N15 (IEC = 1.15 meq g^{-1}), AMPE-M15N15 (IEC = 1.61 meq g^{-1}), AMPE-M15N15 (IEC = 2.08 meq g^{-1}) and AMPE-M20N15 (IEC = 2.69 meq g^{-1}) shows well defined phase separation due to sequential block structure of membranes composed of both hydrophilic (dark) and hydrophobic (bright) domains (Fig. 2(a), (b), (b1) & (c)). These images are recorded in dry state. The size of these domains appears to be small due to the close packing of polymer chain (because of strong intermolecular interactions) [18]. The structural differences between hydrophobic (phenylene sulfo-keto groups) and hydrophilic (tetra quaternary ammonium groups) blocks were responsible for phase separation. Further, with increase in block length of hydrophilic oligomer, the size of dark ionic domains (quaternary ammonium groups containing) also increased and leads to an increment in IEC and hydroxide ion conductivity. Similar effect was

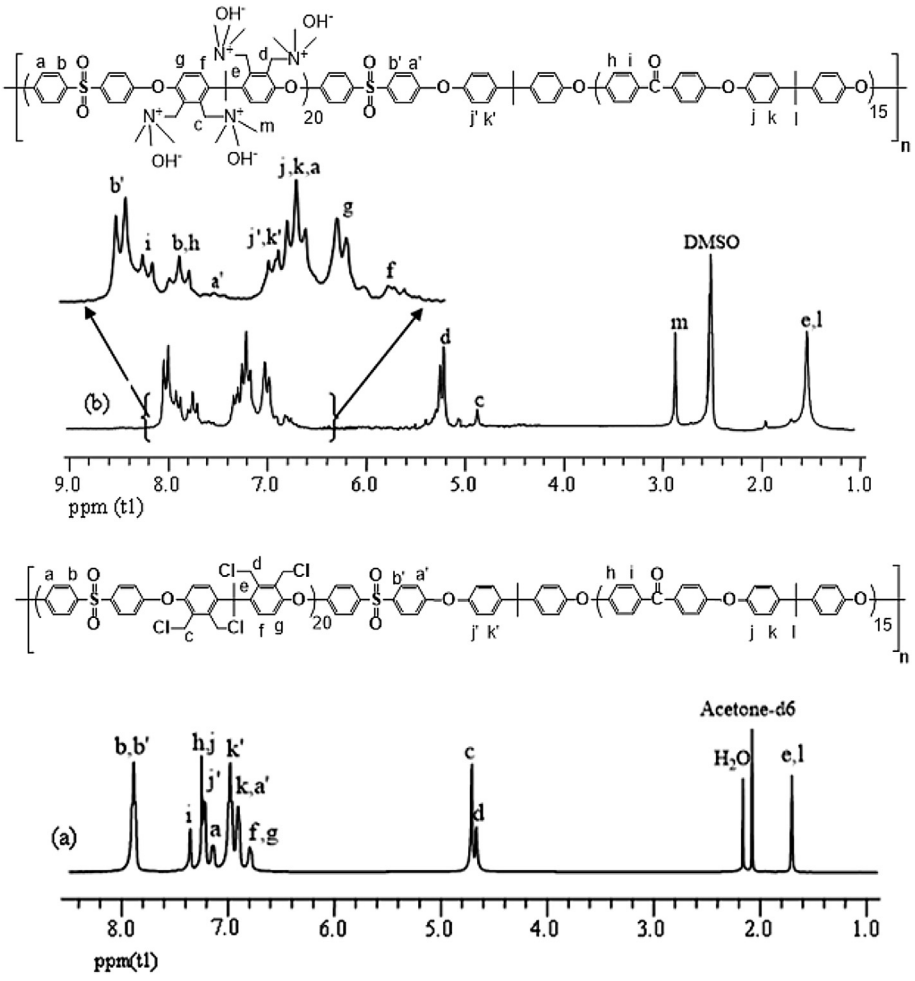

Fig. 1. ^{1}H NMR spectra of (a) CMBPE-M20N15 and (b) AMPE-M20N15 (IEC = 2.69 meq g^{-1}) membranes.

happened in case of AMs with varied DCMs having same hydrophilic/hydrophobic bock length (Fig. 2(b and b1)). This may be due the formation of ionic channels by the interconnected hydrophilic domains and its distribution in the membrane phase [37]. The size of ionic domains increases directly to hydrophilic block length (which improves the water uptake and hydration). Therefore hydration of membrane is directly proportional to hydrophilic block length, the size of ionic domains increases respectively. To assess the ion conducting nature, developed AMs were further characterized for their physic- and electro-chemical properties.

3.5. Ion exchange capacity (IEC), water uptake (WU), through-plane swelling ratio (%) and hydroxide ion conductivity (σ) of AMs

The IEC, *WU*, number of adsorbed water molecules per ammonium groups (λ) and hydroxide ion conductivities of developed AMs with different oligomer lengths and DCMs were summarized in Table 2. Availability of sufficient amount of water in the membrane phase leads to formation of ion conducting channels and thus high hydroxide conductivity (σ), while excess of water uptake (*WU*) causes deformation in the membrane because of excessive swelling. Thus, membrane water uptake and hydroxide ion conductivity are important structural characteristics; measured at 30 °C (Section S3) [38]. It clearly demonstrates the dependency of water uptake and hydroxide conductivities of developed AMs on IEC (Fig. 3(a and b)). The AMPE-M20N15 membrane (90% DCM) showed 2.69 meq g^{-1} IEC; ~89.5% WU; ~18.5 number of water molecules adsorbed per ammonium groups (λ) and 107 mS cm^{-1} hydroxide conductivity. This membrane exhibit about 23.8% through-plane swelling and varies proportionally with hydrophilic block length intimates the formation of ordered hydrophilic domains in the multiblock copolymer. The in-plane swelling does not show much variation with the hydrophilic block length and found to be less than 8.0%. Relatively low *WU* and λ values were observed due to contribution of aromatic sulfo-ether bridge along with hydrophobic block for inhibiting excessive water uptake. The ionic conductivity and IEC values of developed AMPE-M20N15 membrane (IEC = 2.69 meq g^{-1}) was compared with other reported AMs in the literature (Table S3). Alteration in anion exchange membrane conductivities because of CO_2 contamination in fuel cell operation is also expected. Thus, membrane conductivities were also recorded in HCO_3^- form and included in Table 2. Marginal deterioration in conductivity was observed due to less mobility of HCO_3^- in compared with OH^- form. Temperature dependence of hydroxide ion conductivities of different AMPE membranes in OH^- form (Fig. S3) were clearly demonstrates the increase in conductivity with respect to temperature. The AMPE-M20N15 (IEC = 2.69 meq g^{-1}) membrane exhibited very high conductivity of ~150 mS cm^{-1} at 80 °C was observed due to formation of ion transport channels by highly functionalized blocks through phase separated morphology. Further, these multiblock AMPE membranes showed IEC dependent activation energy (6–11 kJ mol^{-1})

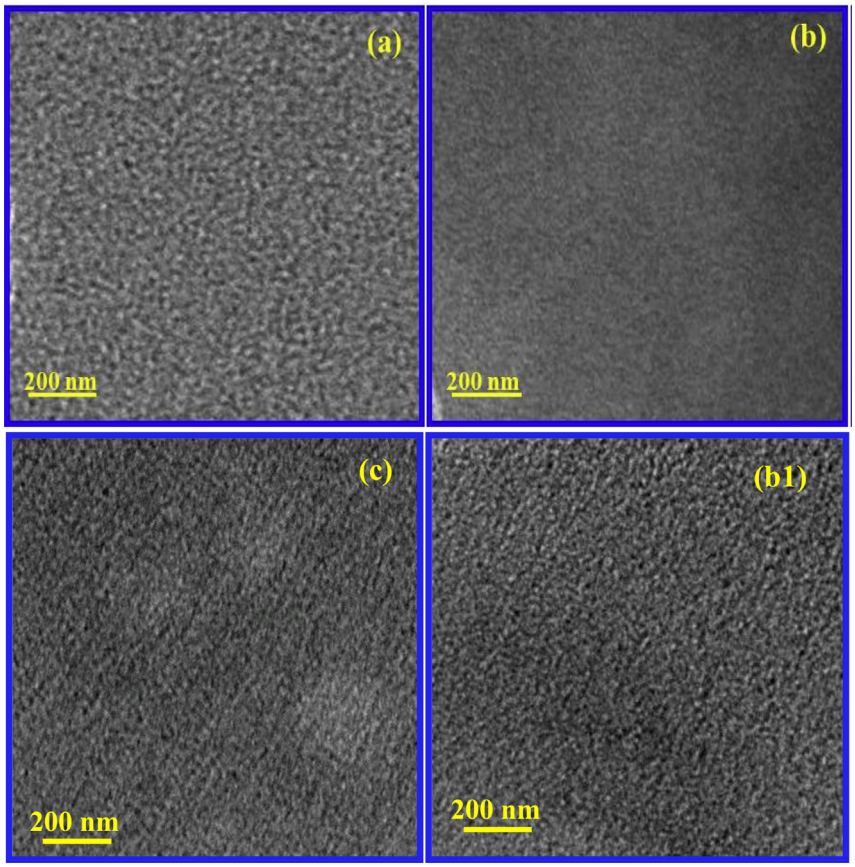

Fig. 2. TEM images of developed AMs having different hydrophilic blocks: (a) AMPE-M10N15 (IEC = 1.15 meq g^{-1}); (b) AMPE-M15N15 (IEC = 1.61 meq g^{-1}); (c) AMPE-M20N15 (IEC = 2.69 meq g^{-1}); and (b1) AMPE-M15N15 (IEC = 2.08 meq g^{-1}) membranes.

may be due to inter-linked hydrophilic channels responsible for fast ion/molecule diffusion/conduction. These results indicate multi-block structures with highly functionalized blocks are effective for improved hydroxide conductivity and IEC.

3.6. Alkaline stability and durability

During fuel cell application, chemical instability of AMs under hydrothermal (or) alkaline conditions is a challenging issue [18,39–41]. The AMPE-M20N15 (IEC = 2.69 meq g^{-1}) membrane was treated in hot water at 80 °C for 500 h, and change in their chemical structure was analysed by ^{1}H NMR spectra (Fig. S5). Treated AMPE-M20N15 (IEC = 2.69 meq g^{-1}) membrane exhibits slightly smaller peaks for the methyl and methylene protons in compare with pristine membrane. The slight shift in δ-values of aromatic protons leads to merging; caused by less deterioration. Generally, AMs degradation occurs due to the effective nucleophilic (OH^-) attack on the quaternary ammonium group of the membrane matrix. Degradations such as Sommelet–Hauser rearrangement and Hofmann elimination are avoided due to the absence of ortho- and β-hydrogen atoms respectively. The suppressed nucleophilic (OH^-) attack (due to steric hindrance effect of two bulky vicinal quaternary ammonium groups) leads to Stevens rearrangement and S_N2 substitution reactions caused for less degradation. Despite of less degradation in the membrane matrix, further investigation is in progress to completely avoid these degradations in alkaline

Table 2
Variation of IEC, water uptake, through-plane swelling ratio (%), number of adsorbed water molecules (λ), ion conductivity (σ) of different AMPE membranes.

DCM (%)	Membrane	IEC[a] (meq g^{-1})	IEC[b] (meq g^{-1})	WU (%)	Through-plane swelling ratio (%)	λ[c]	σ (mS cm^{-1}) at 30 °C	
							$-OH^-$ form	$-HCO_3^-$ form
35	AMPE-M10N15	1.15	1.09	21.5	8.4	10.4	28.2	18.5
	AMPE-M15N15	1.35	1.33	39.6	11.9	16.3	34.4	25.3
	AMPE-M20N15	1.60	1.56	53.1	13.2	18.3	60.0	36.7
55	AMPE-M10N15	1.39	1.28	36.0	12.6	14.4	39.5	26.2
	AMPE-M15N15	1.61	1.58	49.9	14.1	17.5	54.5	43.0
	AMPE-M20N15	1.92	1.95	67.9	18.6	19.7	82.0	70.1
90	AMPE-M10N15	1.72	1.65	58.9	17.3	19.0	67.7	39.3
	AMPE-M15N15	2.08	1.97	72.2	19.5	19.3	86.0	72.8
	AMPE-M20N15	2.69	2.64	89.5	23.8	18.5	107.0	85.4

[a] Calculated from the DCM and the copolymer composition.
[b] Estimated from the ^{1}H NMR spectra of AMPE membranes.
[c] Number of adsorbed water molecules calculated from the equation, $\lambda = [WU \times 1000]/[18 \times IEC\ (meq\ g^{-1})]$.

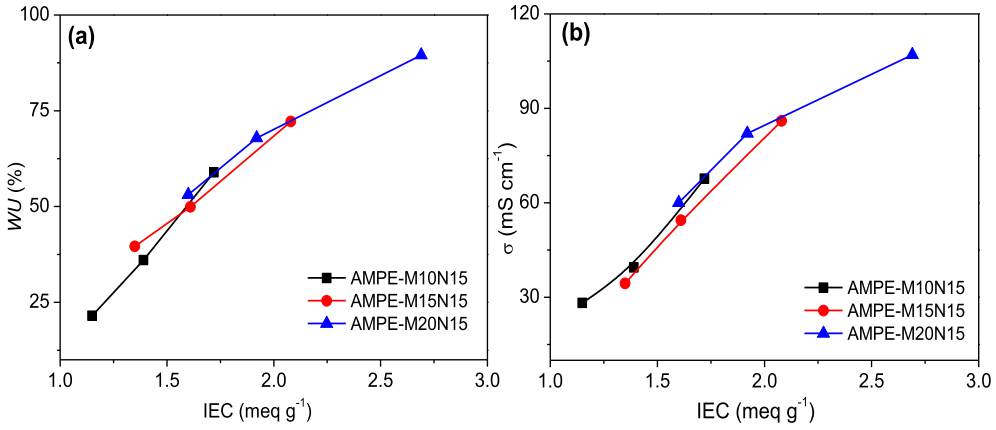

Fig. 3. (a) Water uptake (%) and (b) hydroxide conductivity as a function of IEC at 30 °C: (triangle = M20N15, circle = M15N15, square = M10N15).

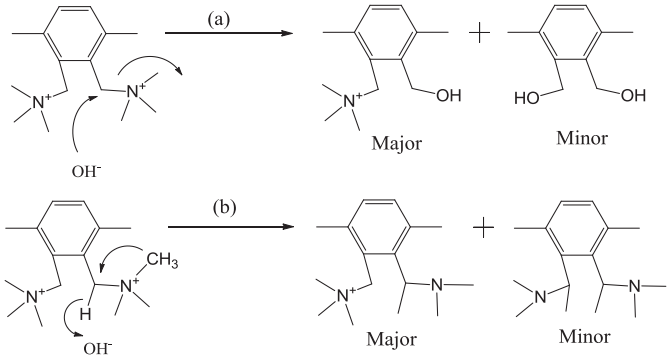

(a) Nucleophillic substitution reaction, (b) Stevens Rearrangement

Fig. 4. Possible degradation mechanism of developed AMs.

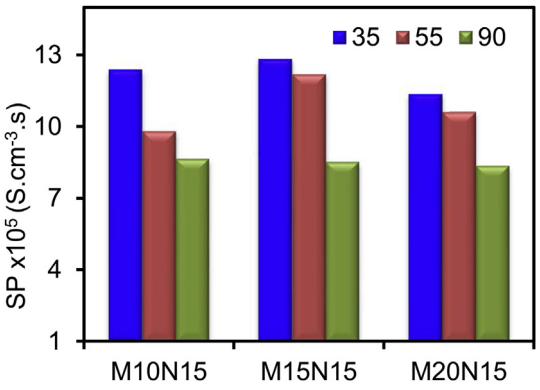

Fig. 6. Selectivity parameter (SP) values of developed AMs at 60 °C.

media. Possible degradation mechanisms of these AMs are included in Fig. 4.

The durability of the AMPE-M20N15 membranes (different DCMs) was investigated by recording their hydroxide ion conductivity and IEC at different time intervals during 500 h treatment with 8 M NaOH at 80 °C (Fig. 5). Even after 500 h treatment, these membranes retained 85% IEC and 80% conductivity along with their toughness and flexibility. Chemical structures before and after the complete treatment were also analysed by ^{1}H NMR spectra (Fig. S6). The peak intensities of both methyl and methylene protons were slightly lowered after treatment and observed less deterioration in spite of having maximum number of quaternary ammonium groups. This deterioration in IEC and conductivity was consistent with each other. Since membrane conductivity attained constant value after several hours, high durability of AMPE membranes appears to be very promising for ADMFCs application.

3.7. Methanol permeability and selectivity parameter

The methanol tolerance and selectivity (the ratio of the hydroxide conductivity to the methanol permeability) was investigated by developed AMs in 2 M MeOH at 60 °C which is about the ADMFC

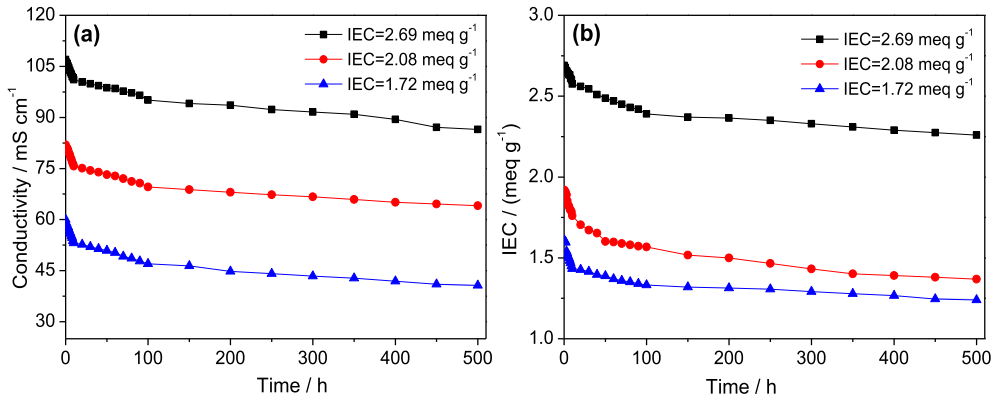

Fig. 5. Variation of (a) hydroxide conductivity and (b) IEC of developed AMPE-M20N15 membranes as a function of time under alkaline treatment in 8 M NaOH at 80 °C.

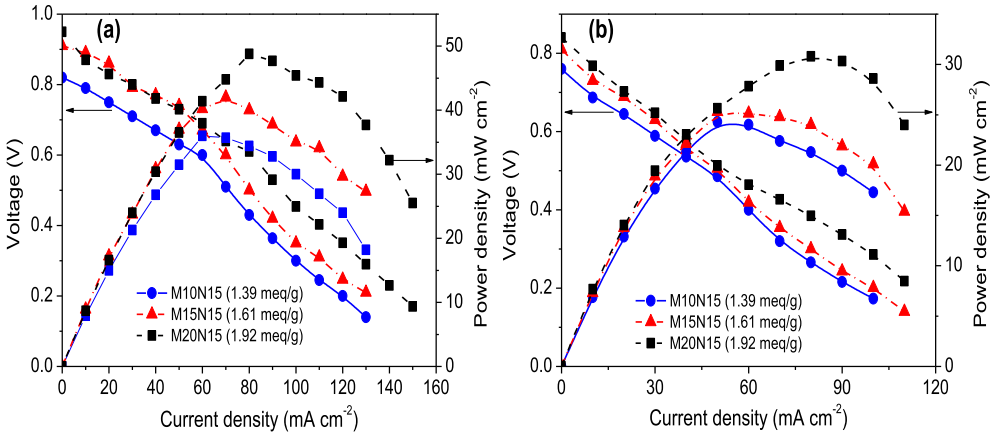

Fig. 7. Fuel cell performance of developed AMs at 65 °C: (a) before and (b) after alkaline treatment.

operating temperature (Fig. 6) by our previous method; compared with other ADMFC membranes [43]. The methanol permeability values increases along with hydrophilic block length as well as degree of functionality. The methanol permeability of developed AMs showed reasonable values (3.29–16.64 × 10^{-8} cm^2 s^{-1}) in spite of high conductivity, may be due to the amination of membrane matrix led to a decrease in free void volume which is responsible for mass transport [42]. Prepared AMPE-M20N15 (1.92 meq g^{-1}) membrane exhibits 10.6 × 10^{-8} cm^2 s^{-1} methanol permeability at 60 °C. This value can be compared with other alkaline membranes reported in the literature (Table S4).

The developed AMs showed higher SP values (8.3 × 10^5 S cm^{-3} s to 12.8 × 10^5 S cm^{-3} s) in compare with that of Nafion117 (0.72 × 10^5 S cm^{-3} s) at 60 °C [43]. The selectivity decreases respectively with the increase of hydrophilic block length may be due to the formation of ionic channels which enhances methanol permeability. But the conductivity increases proportionally with respect to hydrophilic block length. As the selectivity parameter values depends on both conductivity and methanol permeability, developed membranes showed high conductivity values which ignores the enhancement of methanol permeability leads to high selectivity parameter values. The higher selectivity is the potentiality of AMs for ADMFC application.

3.8. Single cell performance of developed AMs

Fig. 7(a) shows the polarization curves for different AMs (M10N15 (1.39 meq g^{-1}), M15N15 (1.61 meq g^{-1}) and M20N15 (1.92 meq g^{-1})) in single cell ADMFC with 2 M MeOH in 6 M NaOH at 65 °C. M20N15 membrane showed 0.95 V OCV and 48.8 mW cm^{-2} power density at 80 mA cm^{-2} current density. These developed membrane exhibits higher peak power density values with other AMs (Table S4). High OCV for M20N15 membrane was attributed to the less fuel loss (reverse electro-osmosis), high membrane conductivity and better kinetics in alkaline medium. OCV and power density increased with hydrophilic block length (Fig. 7(a)) may be due to increase in IEC and hydroxide conductivity. After alkaline stability test for AMs, their polarization curves were also recorded under similar conditions (Fig. 7(b)), to assess if any deterioration in membrane performance. After the long-time alkaline treatment, these membranes exhibited low OCV (0.76–0.84 V) and power density (24.3–30.8 mW cm^{-2}) in compare with fresh membrane. The degradation in cell performance was attributed to the deterioration in functional groups of the matrix under long term alkaline medium due to Stevens rearrangement and S_N2 substitution reaction. These observations revealed potential applications of developed AMs for ADMFCs.

4. Conclusions

TCMBP monomers with 90–35% DCMs are synthesized by a facile method. A series of aminated multiblock poly(arylene ether)s with different hydrophilic block lengths were also synthesised by nucleophilc substitution poly condensation of TCMBP, 4,4′-difluorophenyl sulfone and 4,4′-difluorobenzophenone monomers followed by Menshutkin reaction, avoids the use of CMME. The AMPE-M20N15 membrane (DCM-90%) show 2.69 meq g^{-1} IEC and 107 mS cm^{-1} hydroxide ion conductivity at 30 °C. Morphological studies of these membranes reveal distinct hydrophilic and hydrophobic phase separation. Alkaline stability along with durability of AMPE membranes is also examined to assess their suitability for ADMFCs. Under single cell performance evaluation in alkaline medium, M20N15 membrane exhibit about 0.95 V OCV and 48.8 mW cm^{-2} power density at 80 mA cm^{-2} current density. Further, fuel cell performance studies of long term alkaline treated membranes shows marginal deterioration and suitability of prepared AMs for ADMFC applications.

Designing concept of these AMs provides an alternate simple route, which enables to introduce high density of functional groups (responsible for high hydroxide conductivity and IEC) without sacrificing the stabilities. Furthermore, reporting reaction also can be used for functionalization of aromatic polymers during the preparation of alkaline membrane for diversified electro-membrane processes.

Acknowledgements

CSIR-CSMCRI Communication No. 107; dated: September. 30, 2013.

Financial assistance received from the Ministry of New and Renewable Energy (MNRE) (project no. 102/79/2010-NT, dated 06 January, 2012), Government of India has been gratefully acknowledged. Instrumental support received from the Analytical Science Division, CSIR-CSMCRI is also gratefully acknowledged.

Appendix A. Supplementary data

Supplementary data related to this article can be found at http://dx.doi.org/10.1016/j.jpowsour.2014.05.129.

References

[1] W. Vielstich, Handbook of Fuel Cells, Wiley, Chichester, England, 2009.
[2] M.A. Hickner, H. Ghassemi, Y.S. Kim, B.R. Einsla, J.E. McGrath, Chem. Rev. 104 (2004) 4587–4612.

[3] G. Couture, A. Alaaeddine, F. Boschet, B. Ameduri, Prog. Polym. Sci. 36 (2011) 1521–1557.
[4] J. Sanabria-Chinchilla, K. Asazawa, T. Sakamoto, K. Yamada, T. Tanaka, P. Strasser, J. Am. Chem. Soc. 133 (2011) 5425–5431.
[5] Y. Zha, M.L.D. Miller, Z.D. Johnson, M.A. Hickner, G.N. Tew, J. Am. Chem. Soc. 134 (2012) 4493–4496.
[6] N. Li, Q. Zhang, C. Wang, Y.M. Lee, M.D. Guiver, Macromolecules 45 (2012) 2411–2419.
[7] K. Kneifel, Desalination 34 (1980) 77–95.
[8] L. Wu, T. Xu, D. Wu, X. Zheng, J. Membr. Sci. 310 (2008) 577–585.
[9] G. Wang, Y. Weng, D. Chu, D. Xie, R. Chen, J. Membr. Sci. 326 (2009) 4–8.
[10] J.R. Varcoe, R.C.T. Slade, E.L.H. Yee, S.D. Poynton, D.J. Driscoll, D.C. Apperley, Chem. Mater. 19 (2007) 2686–2693.
[11] M. Mamlouk, J.A. Horsfall, C. Williams, K. Scott, Int. J. Hydrogen Energy 37 (2012) 11912–11920.
[12] S. Singh, A. Jasti, M. Kumar, V.K. Shahi, Polym. Chem. 1 (2010) 1302–1312.
[13] Y. Xiong, Q.L. Liu, A.M. Zhu, S.M. Huang, Q.H. Zeng, J. Power Sources 186 (2009) 328–333.
[14] Y. Wu, C. Wu, J.R. Varcoe, S.D. Poynton, T. Xu, Y. Fu, J. Power Sources 195 (2010) 3069–3076.
[15] Z. Xia, S. Yuan, G. Jiang, X. Guo, J. Fang, L. Liu, J. Qiao, J. Yin, J. Membr. Sci. 390–391 (2012) 152–159.
[16] D. Aili, M.K. Hansen, R.F. Renzaho, Q. Li, E. Christensen, J.O. Jensen, N.J. Bjerrum, J. Membr. Sci. 447 (2013) 424–432.
[17] M. Tanaka, M. Koike, K. Miyatake, M. Watanabe, Macromolecules 43 (2010) 2657–2659.
[18] M. Tanaka, K. Fukasawa, E. Nishino, S. Yamaguchi, K. Yamada, H. Tanaka, B. Bae, K. Miyatake, M. Watanabe, J. Am. Chem. Soc. 133 (2011) 10646–10654.
[19] M. Tanaka, M. Koike, K. Miyatake, M. Watanabe, Polym. Chem. 2 (2011) 99–106.
[20] M.R. Hibbs, M.A. Hickner, T.M. Alam, S.K. McIntyre, C.H. Fujimoto, C.J. Cornelius, Chem. Mater. 20 (2008) 2566–2573.
[21] J. Wang, S. Li, S. Zhang, Macromolecules 43 (2010) 3890–3896.
[22] X. Li, Q. Liu, Y. Yu, Y. Meng, J. Mater. Chem. A 1 (2013) 4324–4335.
[23] J. Zhou, M. Unlu, J.A. Vega, P.A. Kohl, J. Power Sources 190 (2009) 285–292.
[24] A.A. Zagorodni, D.L. Kotova, V.F. Selemenev, React. Funct. Polym. 53 (2002) 157–171.
[25] V. Neagu, I. Bunia, I. Plesca, Polym. Degrad. Stab. 70 (2000) 463–468.
[26] S. Gu, R. Cai, T. Luo, Z.W. Chen, M.W. Sun, Y. Liu, G.H. He, Y.S. Yan, Angew. Chem. Int. Ed. 48 (2009) 6499–6502.
[27] N. Li, Y. Leng, M.A. Hickner, C.Y. Wang, J. Am. Chem. Soc. 135 (2013) 10124–10133.
[28] US Department of Health Human Services. Public Health Service, National Toxicology Program, Report on Carcinogens, twelfth ed., 2011. http://ntp.niehs.nih.gov/ntp/roc/twelfth/roc12.pdf.
[29] K. Verschueren, Handbook of Environmental Data on Organic Chemicals, second ed., 1983, p. 1310.
[30] K.C. Ma, D. Mackay, S.C. Lee, W.Y. Shiu, Handbook of Physical–Chemical Properties and Environmental Fate for Organic Chemicals, second ed., 2006, pp. 2259–2471.
[31] S. Laskin, M. Kusschner, R.T. Drew, V.P. Capiello, N. Nelson, Arch. Environ. Health 23 (1971) 135–136.
[32] D. Chen, M.A. Hickner, Macromolecules 46 (2013) 9270–9278.
[33] N.J. Robertson, H.A. Kostalik IV, T.J. Clark, P.F. Mutolo, H.D. Abruna, G.W. Coates, J. Am. Chem. Soc. 132 (2010) 3400–3404.
[34] D. Chen, M.A. Hickner, ACS Appl. Mater. Interfaces 4 (2012) 5775–5781.
[35] E. Avram, M.A. Brebu, A. Warshawsky, C. Vasile, Polym. Degrad. Stabil. 69 (2000) 175–181.
[36] X. Yan, G. He, S. Gu, X. Wu, L. Du, H. Zhang, J. Membr. Sci. 375 (2011) 204–211.
[37] C. Wang, N. Li, D.W. Shin, S.Y. Lee, N.R. Kang, Y.M. Lee, M.D. Guiver, Macromolecules 44 (2011) 7296–7306.
[38] A. Jasti, V.K. Shahi, J. Mater. Chem. A 1 (2013) 6134–6137.
[39] J.R. Varcoe, R.C.T. Slade, Fuel Cells 5 (2005) 187–200.
[40] O.I. Deavin, S. Murphy, A.L. Ong, S.D. Poynton, R. Zeng, H. Herman, J.R. Varcoe, Energy Environ. Sci. 5 (2012) 8584–8597.
[41] Y.J. Wang, J. Qiao, R. Baker, J. Zhang, Chem. Soc. Rev. 42 (2013) 5768–5787.
[42] T.D. Nguyen, K. Chan, T. Matsuura, S. Sourirajan, Ind. Eng. Prod. Res. Dev. 23 (1984) 501–508.
[43] A. Jasti, S. Prakash, V.K. Shahi, J. Membr. Sci. 428 (2013) 470–479.

List of symbols

WU: water uptake
σ.: membrane conductivity (mS cm^{-1})
E_a: energy of activation (kJ mol^{-1})
R: gas constant (J K^{-1} mol^{-1})
T: absolute temperature (K)
P: methanol permeability (cm^2 s^{-1})
δ: chemical shift (ppm)
λ: number of adsorbed water molecules
Δx: membrane thickness (cm)
A: membrane conducting area (m^2)
SP: Selectivity parameter (S s cm^{-3})
R^m: membrane resistance (Ω)